Mon. Not. R. Astron. Soc. **000**, 1–17 (0000) Printed 1 February 2008 (MN LATEX style file v1.4)

ASTRO-F - The next generation of mid-infrared surveys

C. P. Pearson[1⋆], H. Matsuhara[1] T. Onaka[2], H.Watarai[1] and T. Matsumoto[1]
[1] *Institute of Space and Astronautical Science, Yoshinodai 3-1-1, Sagamihara, Kanagawa 229 8510, Japan*
[2] *Department of Astronomy, School of Science, University of Tokyo, Tokyo 113-0033, Japan*

Accepted .
Received ;
in original form 2000 June 23

arXiv:astro-ph/0008472v4 5 Feb 2001

ABSTRACT

We present basic observational strategies for ASTRO-F (also known as the Imaging Infra Red Surveyor (IRIS)) to be launched in 2004 by the Japanese Institute of Space and Astronautical Science (ISAS). We examine 2 survey scenarios, a deep ∼1sq.deg. survey reaching sensitivities an order of magnitude below all but the deepest surveys performed by ISO in the mid-IR, and a shallow ∼18sq.deg mid-infrared (7-25μm in 6 bands) covering an area greater than the entire area covered by all ISO mid-IR surveys. Using 2 cosmological models the number of galaxies predicted for each survey is calculated. The first model uses an enhancement of a *classical* $(1+z)^{3.1}$ pure luminosity evolution model (Pearson & Rowan-Robinson 1996). The second model incorporates a strongly evolving ULIG component. For the deep survey, between 20,000-30,000 galaxies should be detected in the shortest wavebands and ≈5000 in the longest (25μm) band. It is predicted that the shallow survey will detect of the order of 100,000 - 150,000 sources. We find that for both ASTRO-F and other small aperture space telescopes, confusion due to faint sources may be severe, especially at the longest mid-IR wavelengths. Using the exceptional range of observational options provided by ASTRO-F (9 wavelength filters and spectroscopic ability from 2.2-25μm), we show that by combining the mid-IR observations with the near-IR camera on ASTRO-F, both the different galaxy populations and rough photometric redshifts can be distinguished in the colour-colour plane. In its role as a surveyor (plus near-IR spectroscopic ability) ASTRO-F will complement well the SIRTF space observatory mission.

Key words: ASTRO-F/IRIS – Cosmology: source counts – Infrared: source counts – Galaxies: evolution .

1 INTRODUCTION

Since the launch in 1983 of the extremely successful IRAS mission, infrared astronomy and in particular infrared galaxy surveys, galaxy evolution and cosmology have enjoyed a great deal of exposure and success within the astronomical community. Now rather fittingly, a year after the 20th anniversary of the launch of IRAS the Japanese infrared space telescope ASTRO-F is set to take MID-IR surveys to the next generation.

Although similar advances in galaxy evolution have been in other wavebands such as at optical wavelengths (Madau et al. 1996), it has become apparent the infrared-sub-mm regime may in fact hold the key to galaxy evolution. The main constraint with optical surveys (HST and ground based) is the extinction due to dust that conceals much of the star formation history of the Universe from optical eyes. At infrared wavelengths the Universe becomes relatively transparent to these extinction and absorption effects providing a unique opportunity to study the star formation history of the Universe relatively unhindered. Furthermore, the recent development of large format infrared arrays combined with a wide field-of-view and high spatial resolution has now been now realized and much better sensitivity than ground-based instruments can be achieved, since observations from space with a cooled telescope do not suffer from any atmospheric and instrument thermal background radiation (especially in the mid-infrared).

Although the emission from dust due to star formation peaks in the wavelength region between 60-100μm a significant fraction, about 40 percent, of the luminosity of starburst galaxies is radiated in the mid-infrared region from

⋆ further info. contact Chris Pearson (cpp@ir.isas.ac.jp)

© 0000 RAS

8-40μm (Soifer et al. 1987). Furthermore unlike the far-infrared, observations at mid-infrared wavelengths are not so severely constrained by detector array size and resolution.

The IRAS satellite surveyed almost the entire sky at 100, 60, 25 & 12μm, detecting more than 25,000 galaxies and providing a huge legacy of data that until the launch of the Infrared Space Observatory (Kessler et al. 1996), remained the only benchmark from which to study galaxy evolution in the infrared. ISO (Nov. 1995 - May 1998) operated at wavelengths from 2.5-240μm and improved on IRAS by a factor of 1000 in sensitivity and by 100 in angular resolution at 12μm. Although strictly speaking an observatory, ISO performed numerous galaxy surveys from 200μm to 7μm (e.g. Bogun et al. (1996), Puget et al. (1996), Kawara et al. (1998), Flores et al. (1999a), (1999b), Taniguchi et al. (1997), Serjeant et al. (1997), Oliver et al. (2000a), Lindern-Vørnle et al. (2000)).

At 15μm the ISO surveys covered a wide range in both sensitivity and spatial area. The deepest conventional surveys reaching down to fluxes of between 500-100μJy (Elbaz et al. 1999), although fluctuation analysis in the HDF and the use of clusters as lenses to amplify the source fluxes, extended these sensitivities down almost an order of magnitude further to ∼50μJy (Altieri et al. 1999), (Metcalfe et al. 1999).

Following ISO it was hoped that the Wide Field Infrared Explorer (WIRE) satellite would provide the next generation of mid-infrared surveys, covering 170sq.deg. at 12μm down to 1.9mJy with smaller area surveys to deeper fluxes. The tragic loss of the WIRE mission left a damaging *hole* in infrared astronomy. The Space Infra-Red Telescope Facility (SIRTF) due for launch in 2002 (Rieke 2000), covering the wavelength range from 3.6-160μm and spectroscopy from 5-37μm is the next major space infrared telescope although again like ISO before it, SIRTF is officially an observatory. It is hoped that SIRTF and ASTRO-F will complement each other well, both providing their own unique contribution to IR astronomy.

This paper investigates several basic survey strategies possible in the mid-infrared using the Infra-Red Camera on ASTRO-F. In section 2 we introduce the ASTRO-F mission. Section 3 explains the model parameters used to predict the survey source counts. In sections 4 and 5 we predict the outcome of a suite of survey options viable with ASTRO-F and in section 6 we give a summary of the results.

2 ASTRO-F / THE INFRA-RED IMAGING SURVEYOR (IRIS)

2.1 ASTRO-F specifications

ASTRO-F, also known as the Infra-Red Imaging Surveyor (IRIS, (Murakami 1998)) will be the second infrared astronomy mission of the Japanese Institute of Space and Astronautical Science (ISAS). ASTRO-F will be a 70cm cooled telescope and will be dedicated for infrared sky surveys (Onaka, Sugiyama, & Miura 1998). ASTRO-F was preceded by the Infra-Red Telescope in Space, IRTS (Murakami et al. 1996), a short 4 week mission during 1995 optimized to measure the diffuse IR emission/background from 1.5-800μm (Matsumoto et al. 2000).

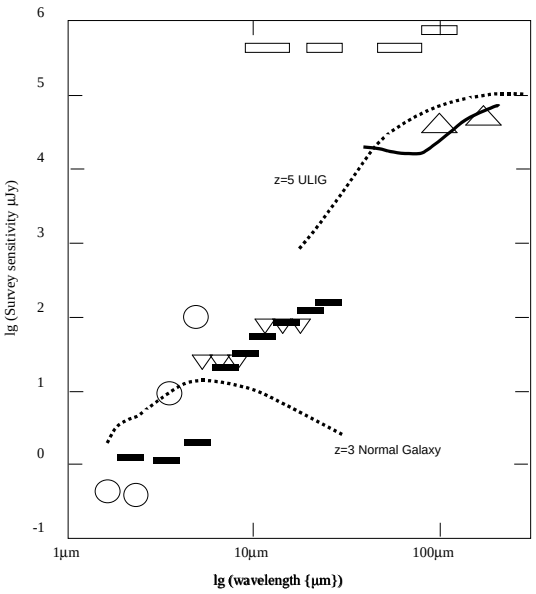

Figure 1. ASTRO-F survey sensitivities (5σ) in comparison with other IR detection limits. ASTRO-F FIS and IRC, assuming a 500s integration (*solid line and filled boxes*), IRAS (*empty boxes*), ISOPHOT (*large upward triangles*), ISOCAM Hubble Deep Field survey limits (Goldschmidt 1997) (*small downward triangles*) and the Japanese Subaru telescope (*unfilled circles*).

The ASTRO-F Ritchey-Chertien telescope has a 70cm aperture and is cooled to 6K (the detectors to 1.8K), using a light weight liquid Helium cryostat. The temperature of the outer wall of the cryostat is expected to be maintained below 200K via radiation cooling. Two 2-stage Stirling-cycle coolers ensure minimum heat flow from the outer wall of the cryostat, almost doubling the lifetime of the Helium thus allowing approximately 150l of liquid Helium to sustain the telescope for more than 500 days. Another advantage of using the mechanical coolers is that the near-infrared detectors will still be usable even after the Helium expires (providing the coolers continue to function). The primary and secondary light-weight mirrors (only 11kg) have been made from silicon carbide, adopted due to its large Youngs modulus and high thermal conductivity.

ASTRO-F covers a wide wavelength range from the K-band to 200μm. Two focal-plane instruments are installed. One is the Far-Infrared Surveyor ((Kawada 1998) (Takahashi et al. 2000)) which will survey the entire sky in the wavelength range from 50 to 200μm with angular resolutions of 30 - 50 arcsec using high sensitivity Ge:Ga detector arrays (see Takeuchi et al. (1999) Pearson et al.(in preperation) for FIS survey predictions). The FIS also has a Fourier-transform spectrometer with a resolution of $0.5cm^{-1}$ allowing imaging spectroscopy of selected sources. The other focal-plane instrument is the Infrared Camera (IRC, see Table 1 (Matsuhara 1998),(Watarai et al. 2000)). It employs large-format detector arrays and will take deep images of

selected sky regions in the near-infrared and mid-infrared range. ASTRO-F will have a much higher sensitivity than that of the IRAS survey. For example, ASTRO-F has 50 - 100 times higher sensitivity at 100μm and more than 1000 times that at mid-infrared wavelengths. The detection limits are 1-100 mJy in the near-mid infrared and 10-100mJy in the far-infrared (Fig. 1). ASTRO-F will also offer 4 times the resolution over 10 times the detector area compared to ISOCAM on ISO. Although similar sensitivities are also capable with SIRTIF (Fazio et al. 1998), ASTRO-F will be able to reach such limits over a wider area (10-20sq. deg. due to the larger FOV) in the mid-infrared and the entire sky at far-infrared wavelengths. At 2.5-5 years, SIRTF has a longer projected lifetime than ASTRO-F, it has no spectroscopic capability at near-infrared wavelengths ($< 5\mu m$). ASTRO-F has this added capability and will in fact be able to continue to use this instrument even after liquid Helium exhaustion.

With the ASTRO-F surveys, great progress is expected in the fields of galaxy evolution, formation of stars and planets, dark matter and brown dwarfs. ASTRO-F is now scheduled to be launched with ISAS's M-V launch vehicle, into a sun-synchronous polar orbit with an altitude of 750 km in mid 2004.

2.2 The Infra-Red Camera (IRC)

The IRC is a wide-field imaging instrument (Matsuhara 1998). It consists of three independent camera systems. IRC-NIR (1.8-5 μm), MIR-S (5-12μm) and MIR-L (10-25μm) - see Table 1 (Watarai et al. 2000). At the focus of these cameras are new large format infrared array detectors (NIR:512x412 InSb, MIR:256x256 Si:As IBC). For IRC-NIR, only a 412 x 412 portion of the InSb array is used to observe the $10'$x $10'$field, the remaining detector area (412x100) being used for a slit spectroscopy via a slit added to the entrance aperture. The advantages of such infrared observations from space are the negligible atmospheric absorption and low background emission (1∼5 photons/s for NIR, and 100∼1000 photons/s for MIR). These 3 channels will have a field of view of $10'$x$10'$. The MIR-S channel shares the FOV with the NIR channel with light of wavelength shorter than 5μm being transmitted to the IRC-NIR and incident light of longer wavelength being reflected to the MIR-S channel, while the MIR-L-IRC FOV is separated by approximately $20'$. At the aperture stop of each camera (i.e., the image position of the telescope primary mirror, ≈11∼12mm in diameter), the observing wavelength is selected by a filter wheel. The filter bands are selected by rotating the filter wheels. The IRC-NIR filter wheel has 6 positions. 3 bandpass filters of Ge substrates (6mm thick), 2 dispersive elements and a blank mask. The 3 band pass filters of the MIR-S are made of ZnS substrates of 7mm thickness and the grism (used for spectroscopy) has 4.8 grooves per mm. The spare filter wheel position (TBD) will be another grism or a broad band filter. The MIR-L channel is located $25'$ away from the telescope axis and has 4 filters on CdTe substrates of 8mm thickness plus a grism (2.5 grooves/mm) and a spare as yet undecided position for possibly another grism or a broad band filter.

In addition to the narrow-band photometric filter bands, there is also a blank position to measure the dark level, and positions for grisms. Thus the IRC also has the capability of low-dispersion spectroscopy by replacing the filters with the grisms attached to the filter wheels. This spectroscopic capability will be used to classify detected sources, to obtain source SED's and to roughly estimate their redshifts. There also exists one spare position on the filter wheel that is as yet undecided but could possibly be utilized as a another grism or a broad band filter.

The IRC will be operated under pointing mode where the satellite attitude is fixed for ≈10 minutes in order to observe one target direction on the sky, the typical exposure time per pointing being 500 seconds in total. Such pointing observations can be made 1-3 times per revolution of the satellite. For the in-flight calibration of detector response and flat-fielding, a light source with uniform intensity is also included. Illumination of a rough light-scattering surface of a blank position on the filter wheel facing the detector array before and after each pointing observation will establish the flat-fielding with about 1% accuracy. However, for the MIR cameras, a flat-field accuracy better than 0.1% is required. Therefore each pointing observation (≈10 minutes) is divided into 8∼10 independent observations in units of the exposure time of the IRC-NIR (≈ 62s, 60s for a dark sky and 2s exposure for observation of bright sources in the case of the NIR-IRC and 6x10 + 2x1s for the MIR-IRC (Watarai et al. 2000)), with the telescope position on the sky being moved by $5''$∼$30''$from the origin of the observing field among the sub-observations.

3 MID-INFRARED MODEL PARAMETERS

Galaxy source counts are simulated by using an extended and improved evolution of the Pearson and Rowan-Robinson model (Pearson & Rowan-Robinson 1996). The model utilizes a 4 component parameterization based on the IR colours of IRAS galaxies (Rowan-Robinson & Crawford 1989). The model consists of a normal galaxy (IR cirrus like) component defined by cool 100/60μm colours, a starburst component defined by warm 100/60μm colours extending to a high luminosity tail ($L_{60\mu m} >\sim 10^{12} L\odot$) in the IR luminosity function to model the ultraluminous infrared galaxy population (Sanders & Mirabel 1996) and an AGN (Seyfert/QSO 3-30μm dust torii) component (Rowan-Robinson 1995). Components are distinguished on a basis of SED and luminosity class. The composite cool and warm 60μm luminosity functions of Saunders et al. (1990) are used to represent the normal, starburst and ULIG galaxies respectively. The *cool* galaxies are defined in νL_ν from $lgL_{60\mu m} = 6-11.5L\odot$, the starbursts from $lgL_{60\mu m} = 6-12L\odot$ and the ULIG component from $lgL_{60\mu m} > 12L\odot$. The AGN luminosity function is defined from $lgL_{12\mu m} = 8-14L\odot$ at 12μm (Rush, Malkan & Spinoglio 1993) using the luminosity function of Lawrence et al. (1986). To shift the luminosity function from the wavelength at which the luminosity function is defined, λ_{LF}, to the observation wavelength λ_{obs}, the ratio $L(\lambda_{obs})/L(\lambda_{LF})$ is obtained via model template spectra.

K-corrections are calculated using model Spectral Energy Distribution (SED's) templates for each galaxy population. The original model SED's of Pearson & Rowan-Robinson (1996) consisted of normal, starburst, AGN and ultra/hyperluminous galaxy spectra and were found to provide a good fit to IRAS data. However much progress has

Table 1. Infra-Red Camera Parameters

Channel	Wavelength Bands	FOV (Pixel size)
IRC-NIR	K,L,M+$(1.25-2.5, 2-5.5\mu$m grism)	$10'$x$10'(1.4''/pixel)$
IRC-MIR-S	$7, 9, 11\mu$m$(5-10\mu$m grism)	$10'$x$10'(2.34''/pixel)$
IRC-MIR-L	$15, 20, 25\mu$m$(10-25\mu$m grism)	$10'$x$10'(2.34''/pixel)$

been made both in the fields of observation with the Infrared Space Observatory (ISO) and radiative transfer models. Of particular significance for predictions in the mid-infrared region is the inclusion of the so called unidentified infra-red bands probably manifested as Polycyclic Aromatic Hydrocarbons (PAH's (Puget & Leger 1989)), into the model spectra. Such features, prominent in the 6-12μm range would be expected to affect the mid-IR source counts to some extent (Xu et al. 1998). Furthermore, in the wake of the many observations by ISO ((Lu et al. 1997), (Boulade et al. 1996), (Vigroux et al. 1996)), it has become starkly apparent that most galaxies are hosts to such features, with equivalent widths of as much as 10μm, comparable to that of the ISOCAM MIR filter bandpasses (3.5μm & 6μm for the LW2(5-8.5μm) filter and LW3(12-18μm) filters respectively).

The template SED's for the starburst & Ultraluminous *warm* components and the normal *cool* galaxy component are taken from the new models of Efstathiou, Rowan-Robinson & Siebenmorgen (2000) and Efstathiou & Siebenmorgen (2000) respectively, while the AGN SED template is that of Rowan-Robinson (1995). The new starburst galaxy SED's are based on the evolution of optically thick giant molecular clouds, centrally illuminated by massive stars. The starburst models are defined by t , the age of the starburst in Myrs; τ, the initial optical depth (in V) of the molecular clouds; χ, the ratio of radiation field to the local solar neighborhood. The starburst SED can be considered M82 *like*, while the ULIG SED represents an ARP220 type galaxy (c.f. the more extreme hyperluminous galaxy IRAS F10214 (Rowan-Robinson et al. 1993) that was used in the earlier models of Pearson & Rowan-Robinson (1996) to represent the high end of the starburst luminosity function). Exponentially decaying $10^7 \sim 10^8$yrs old starbursts reproduce well the IRAS colours of galaxies and provide good fits to the data for the popular starburst galaxy template M82 and to the recently ISO observed starburst galaxy NGC6090 (Acosta et al. 1996). The new galaxy SED templates also incorporate the full range of PAH features (Siebenmorgen & Krugel 1992) crucial for mid-infrared predications and not previously included in the earlier model SED's (Rowan-Robinson 1992), (Rowan-Robinson & Efstathiou 1993). It should be noted that although the PAH features seem somewhat strong and sharply defined in these models, as long as the energy contained within the peaks is consistent with observations and the SEDs are smoothed and convolved with the filter response function, the general shape of the PAH features is not so critical (see fig. 3).

We consider 2 evolutionary models. The first model may be considered a *safe, well established benchmark* for the survey predictions (we refer to this as the *Levol* (luminosity evolution) model. For this model, simple luminosity evolution of the form $L(z) = L(0)(1+z)^{3.1}$ to a redshift of $z = 2$ is incorporated into the starburst, ULIG, and AGN components. This form of evolution has been shown to provide a good fit to the source counts over a wide range in wavelength (Rowan-Robinson et al. 1999), (Pearson & Rowan-Robinson 1996), (Benn et al. 1993), (Boyle et al. 1988) although additional evolution is almost certainly needed to explain the faintest 15μm ISOCAM & 170μm ISOPHOT source counts (Elbaz et al. 1999), (Elbaz et al. 1999b), (Dole et al. 2000), (Biviano et al. 1999), (Metcalfe et al. 1999), (Altieri et al. 1999) and the SCUBA sub-mm data (Hughes et al. 1998), (Smail, Ivison & Blain 1997), (Blain, Kneib, Ivison & Smail 1999), (Barger, Cowie & Sanders 1999).

The second model incorporates more extreme evolution. In this model, the starburst and AGN evolve *similarly* to the *Levol* model with a power law of $L(z) = L(0)(1+z)^{3.1}$, however, in addition, the high luminosity end of the starburst luminosity function (ULIG population) evolves not only in luminosity but also in number exponentially. We will refer to this model as the *ULIG* model. Although locally ($\approx z < 0.1$), ULIGs have a space density approximately similar to optically selected QSOs, analysis of the IRAS Faint Source catalogue has hinted at much stronger (density) evolution at higher redshifts (to $z \approx 1$) of the form $(1+z)^g$, with $g \approx 7.6 \pm 3.2$ (Kim & Sanders 1998). Similar strong evolution ($g \approx 10$) is also required to fit the deep 15μm ISO source counts (Dole et al. 2000). Using such strong evolution the source counts from sub-mm to NIR wavelengths can be fitted by one consistent model (see Pearson (2000b) for detailed description of these new models).

The strongest constraint on the evolution in the mid-infrared are the source counts at 15μm (Elbaz et al. 1999), where the counts have been measured over 4 orders of magnitude in flux. These counts exhibit a super Euclidean slope at fluxes of around $1mJy$, flattening at fainter fluxes of $0.4mJy$ and are best shown by plotting the differential source counts. Fig. 2 shows the *ULIG* and *Levol* model fits to the 15μm source counts. As can be seen from the figure, although the *Levol* model provides a very good general fit to source counts over a wide range in wavelength (and should therefore not be discarded out of hand by any means (see Serjeant et al. (2000) for a detailed comparison of the Pearson & Rowan-Robinson model with ISO 15 & 6.7μm observations.), it cannot however, reproduce the detail of the dips and peaks observed in the ISO counts. However for a general investigation and prediction of the capabilities of ASTRO-F, this simple evolution will suffice.

Note that although an E/S0 component is not strictly

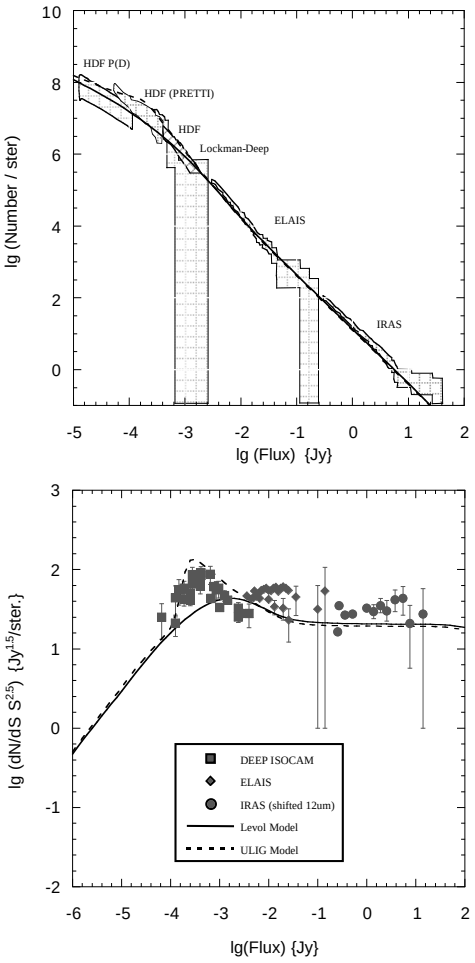

Figure 2. Source counts at 15μm for the *Levol* & *ULIG* models compared with the source counts as observed by ISO. *Top* - Integral source counts compared with observations from Hubble Deep Field (P(D) analysis - Oliver et al. (1997), HDF counts derived using the PRETI method - Aussel et al. (1999), Lockman Hole - Elbaz et al. (1998), ELAIS - Serjeant et al. (2000) and shifted IRAS counts. *Bottom* - Normalized differential counts compared with observations - Elbaz (1999b), Serjeant et al. (2000).

included in the models, the strong evolution in the starburst component adequately compensates for this absence (Pearson & Rowan-Robinson 1996). Furthermore any significant contribution from such a population decreases rapidly towards longer wavelengths. The model assumes $\Omega = 0.1, H_o = 50 kms^{-1} Mpc^{-1}$.

4 MID-INFRARED SURVEYS WITH THE IRC

4.1 The effect of smoothing the SEDs by the filter bandwidths

With the IRC-MIR on ASTRO-F, mid-infrared surveys will be possible over a wide range of wavelengths from 6-25μm. With such a wide range of options and combinations available for mid-infrared surveying, it is of paramount importance that the filters be used in the most efficient way, in order to, for example, detect the most sources or to discriminate between galaxy types or redshift domains. Due to the dominance of the PAH features in the mid-infrared, the filter bandwidth will have a significant effect on the results. A previous, initial estimation of probable survey outcomes made by Pearson (2000a) assumed monochromatic survey filter wavelengths and hence suffered from prominent spikes in the N-z distribution of galaxies due to the effect of the PAH features in the mid-IR (see fig. 8 (a)). The narrow band filters have a resolution, $\Delta\lambda/\lambda = \Delta\nu/\nu = 0.2$. Therefore the template SEDs are convolved with the filter bandwidths at each wavelength to produce a "smoothed" SED template. Such smoothing provides a much more realistic picture of the mid-infrared SED of galaxies as will be seen by ASTRO-F. The smoothed normal and starburst galaxy SED's are shown in Fig. 3. Note that the effect of smoothing the AGN SED is negligible due to the fact that the mid-infrared broadband features are not present in the AGN spectra having been suppressed / destroyed by the intense radiation field in the AGN environment (Lutz et al. 1997), (Roache et al. 1991), (Genzel et al. 1998). The most obvious difference between the smoothed and unsmoothed SED's is the significant reduction of the amplitude of the prominent PAH features which should have the effect of *smoothing* the galaxy *N-z* distributions.

In the following subsections, surveys with this narrow band filter configuration are considered.

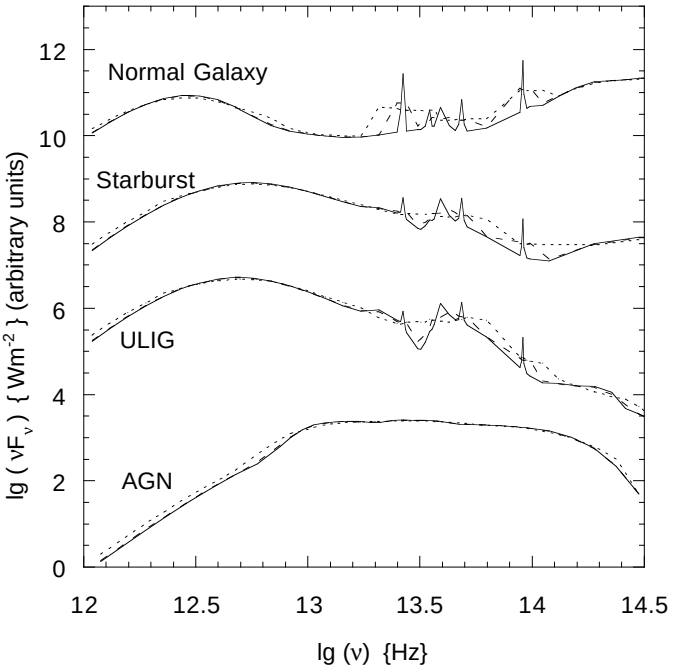

Figure 3. The model SED templates used for the source count models. Also shown is the effect of smoothing the original template SEDs (*solid line*) by the filter bandwidth at each wavelength. In the case of the narrow band filters $\Delta\lambda/\lambda = \Delta\nu/\nu = 0.2$ (*dashed line*). If the wide band filter option is utilized, $\Delta\lambda/\lambda = \Delta\nu/\nu = 0.67$ (*dotted line*)

4.2 Survey strategies and detection limits

Mid-infrared source counts from 7-25μm, corresponding to the IRC-MIR-S and IRC-MIR-L filter wavelengths are shown in detail in fig. 4 and fig. 5 for the *Levol* and *ULIG* models respectively. In general there is an increasing contribution from the starburst (and AGN) component towards longer wavelengths. In the case of the *ULIG* model the source counts at all wavelengths exhibit a hump at the flux where the ULIG component peaks and then consequently flattens.

Table 2 shows the current expected sensitivities for a single pointing (5σ) using the narrow band filters on the IRC-MIR detectors. The confusion limit due to background sources is calculated from the source counts and is also tabulated in table 2. For any space telescope, the confusion limit at mid-infrared wavelengths will be lower than in the far-infrared (and lie at higher redshift) due to the higher spatial resolution at the shorter wavelengths ($\sim \lambda/D$). The confusion limits are calculated from the source counts assuming the classical confusion criteria of a source density of 1 source per 40 beams of the observing instrument, where the beam diameter is given by $d = 1.2\lambda/D$, where D is the telescope diameter (70cm). Here we calculate the source confusion assuming a beam diameter equivalent to the FWHM of the Airy disc, $d = 1.2\lambda/D$ such that the beam diameter at 15μm is $5.3''$corresponding to a source confusion density of ≈14660 sources. The corresponding limiting flux will of course be model dependent.

We investigate 2 general strategies for possible mid-infrared surveys with ASTRO-F.

The first is an ultra-deep survey covering ≈ $3200 sq.arcmin.$ around the North Ecliptic Pole (NEP), making 20 pointings per pixel giving an effective gain of $\sqrt{20}$ over the base sensitivity (given in table 2). The NEP is chosen due to the fact that ASTRO-F will be in a sun-synchronous polar orbit with the sunshield permanently facing inward towards the Sun and the telescope direction always approximately on the plane perpendicular to the direction of the Sun (i.e., toward the pole). Thus a minimal amount of survey planning and telescope moving is required.

The second survey strategy is a wide field shallow survey with a single pointing per pixel covering approximately $20x3200 sq.arcmin. \approx 18^{\square}$. The area covered by the shallow wide field survey would be larger, and the sensitivity ~ 20 times deeper at 15μm than that of the European Large Area ISO Survey (ELAIS (Oliver 2000b) which impressively covered $\sim 12^{\square}$ at 15μm to $\approx 2mJy$ (table 3).

From table 2, it is apparent that such mid-infrared surveys may well be severely constrained by source confusion. In fig. 6 a comparison is made between the survey sensitivities expected for the 3200sq.arcmin. deep NEP survey, the 18sq.deg. shallow (single pointing) survey and the corresponding source confusion limits predicted by the *Levol* and *ULIG* models. Deep surveys with the MIR-S instrument are almost on the confusion limit due to background sources (the optimal position required!), however at the longer wavelengths corresponding to the MIR-L, the surveys is expected to be heavily contaminated by the background source confusion. In the case of a wide field shallow survey, there is a greater dependence on the evolutionary model assumed. Assuming the *Levol* model, all bands are above or on the background confusion limit. However, if the *ULIG* model is assumed, then the MIR-L bands still suffer contamination to some extent in the shallow survey as well as the deep NEP survey. Thus, it is apparent that any future surveys in the mid-infrared will be severely limit by source confusion. Even in the case of ISO, observations in the Hubble deep Field at 15μm down to 255μJy were already reaching the confusion limit (Oliver et al. 1997). For ASTRO-F, the problem of source confusion and subsequent source extraction will be somewhat alleviated by the fact that for the deep NEP survey the observations with the IRC-MIR-S, IRC-MIR-L & IRC-NIR instruments overlap allowing multiple observations at different wavelengths.

The main limitations of the ISO deep surveys were effects caused by flat-fielding noise, glitches and transients (Aussel et al. 1999). Although detailed modelling of these effects and their possible influence on the ASTRO-F IRC surveys is being undertaken, it should be noted that the IR arrays used in the IRC-MIR channels utilize the IBC (impurity band conduction) structure that is superior to the bulk photoconductive detection arrays used in ISOCAM, especially with respect to transient behavior which will enable us to obtain better flat fielding. Furthermore, please note that at each pointing we take 6x(7∼10)=42-60 frames with micro-scanning towards the same field of sky hence for 20 pointings the real redundancy is not 20 but 20x(42-60)=840-1200 (Watarai et al. 2000).

4.3 The 3200sq.arcmin. deep NEP MIR survey

The 3200sq.arcmin. survey would take an extremely deep (32 different IRC pointings each 20 pointings deep) observation around a $\sim 67'$diameter doughnut of width $\sim 10'$(i.e. each pointing has an area of 10×10sq. arcmin, the field of view of the IRC) around the NEP. The aim of this survey would be to image as deep as possible in all mid-infrared bands of the IRC.

In fig. 7 the predicted results for the proposed 3200sq.arcmin. Deep NEP MIR survey are shown as a function of object class (normal, starburst, ULIG and AGN) for both the *Levol* and *ULIG* evolutionary models. Note that the ultraluminous galaxy component for *Levol* model is not included as the expected number of sources are negligible (of the order of < unity for the survey area). In the *Levol* evolutionary model, such objects may be serendipitously discovered and would be expected to be very rare objects, such as for example, the hyperluminous galaxy IRAS F10214+4724 (Rowan-Robinson et al.1991), found at z=2.286 on the limit of the IRAS Faint Source Catalogue. The ASTRO-F deep mid-IR survey is not expected to find such objects since shallow, wide area strategies at longer wavelengths are more efficient for this purpose (Pearson & Rowan-Robinson 1996).

Of the order of 20,000-30,000 sources would be detected with the IRC-MIR-S instrument (7-11μm), the majority of which would be normal galaxies that have relatively strong K-corrections as the near-infrared/optical emission is sampled out to higher redshifts (the 3.3μm UIB feature being sampled at z∼1.1 and the K-band at a redshift of ~ 2.2 for the MIR-S 7μm band). Assuming the *Levol* model, ≈ 4000 starburst galaxies and 4000-7000AGN would be expected in all bands except the longest(20-25μm) where the confusion limit becomes severe. In general the trend is towards an in-

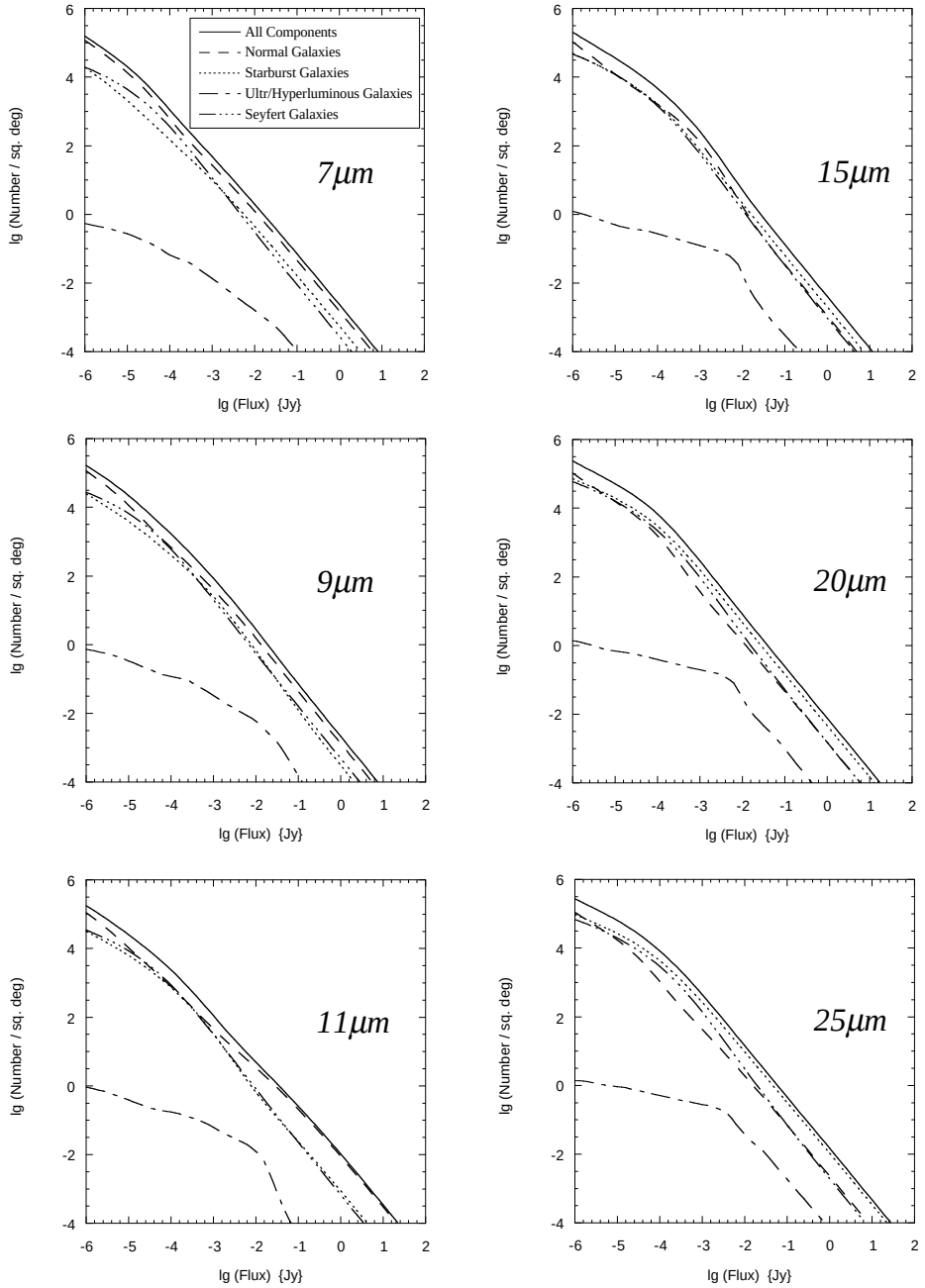

Figure 4. Integral galaxy source counts, assuming the *Levol* model, at 7, 9, 11, 15, 20 & 25μm respectively, corresponding to the IRC-MIR-S and IRC-MIR-L filter wavelengths. Total source counts are shown (*solid line*) with normal (*dash*), starburst (*dot*), ultraluminous galaxy (*dash dot*) and AGN components (*dot-dot-dot-dash*). There is a gradual trend of increasing starburst galaxy contribution towards the longer wavelengths.

creasing fraction of starburst galaxies to normal galaxies towards longer wavelengths. The AGN component maintains an almost constant fraction of the total observed sources over the entire 7-25μm wavelength range.

Fig. 8 shows the number-redshift distributions for the deep NEP survey wavelengths as a function of galaxy component. Predictions for the *Levol (b)* and *ULIG (c)* models are shown. Also for comparison, the N-z distribution for the *Levol (a)* model using source spectra that have *not* been smoothed by the detector bandwidth are also shown. The prominent spikes produced as the PAH features pass through the bands, all but disappear when the SEDs are smoothed. This may have important consequences if the PAH features are hoped to be used as redshift indicators.

The (smoothed) emission from the 3.3μm feature enhances the detectability of the normal galaxy component (and to a similar extent the starburst component) out to redshifts of ∼1-2.5 from 7-11μm respectively. In fact as much

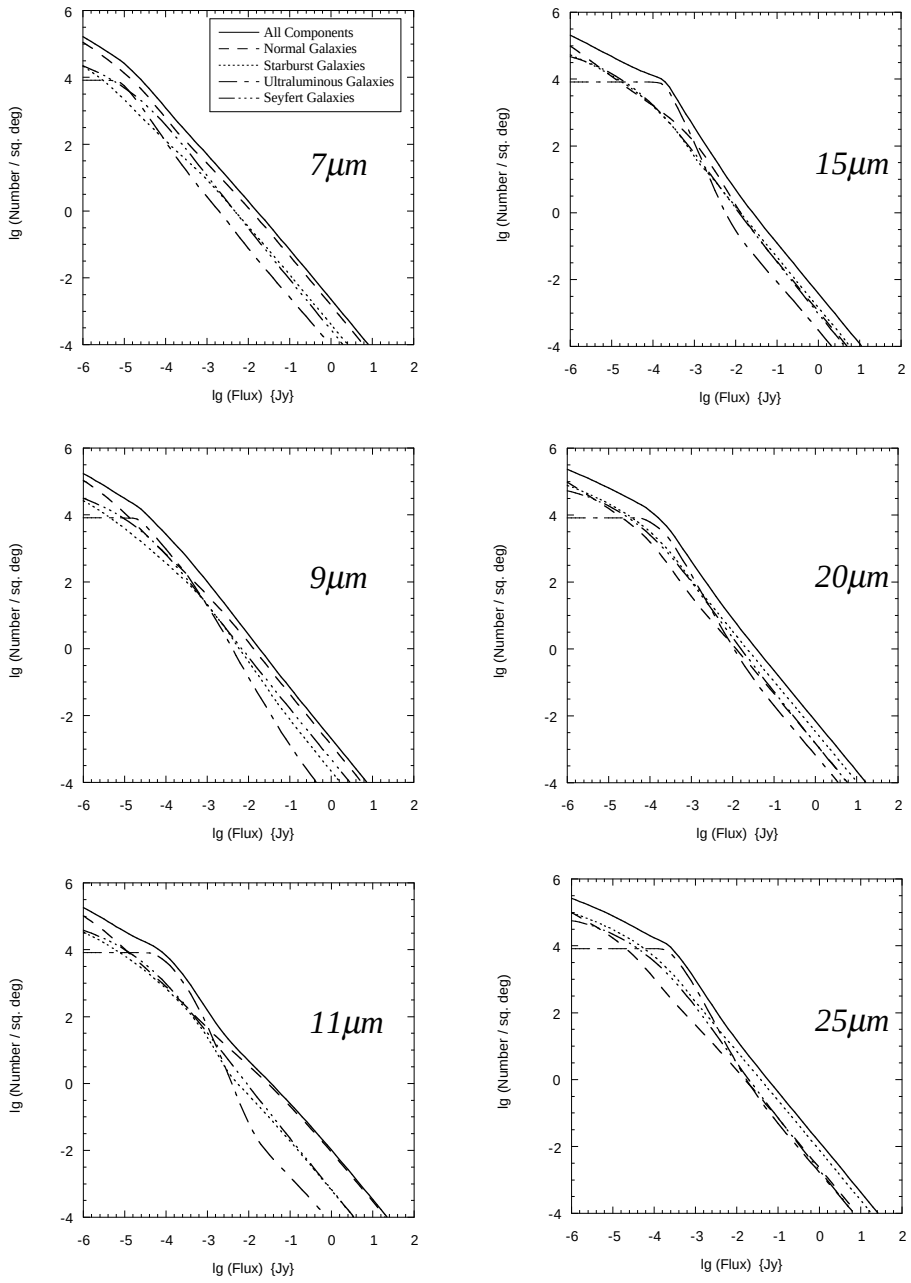

Figure 5. Integral galaxy source counts, assuming the *ULIG* model, at 7, 9, 11, 15, 20 & 25μm respectively, corresponding to the IRC-MIR-S and IRC-MIR-L filter wavelengths. Total source counts are shown (*solid line*) with normal (*dash*), starburst (*dot*), ultraluminous galaxy (*dash dot*) and AGN components (*dot-dot-dot-dash*). Note the predominant bump produced by the strongly evolving ULIG component as compared to the relative scarceness of these sources in the *Levol* model scenario.

as 60% of the normal galaxies may lie at z>1 in the shortest 2 bands. In all bands, approximately 50% of the starburst galaxies lie at z>1 within which ≈10-20% may lie at z>2. Interestingly, the role of the mid-IR PAH features seems rather important enhancing the starburst galaxy population at redshifts of approximately 1 and 2 in the 15 and 20-25μm bands respectively as the mid-infrared region containing the 6-13μm *forest* of PAH features is redshifted into the respective observation windows.

Naturally, the *ULIG* model predicts starkly different results due to the inclusion of the strongly evolving new population. The fraction of ULIGs rises from around 10% in the shortest waveband to 65% in the longest. The number of ULIGs predicted remains approximately constant ∼7000 from 7-15μm, dropping to ∼3000 at the longest wavelengths due in part to the lower sensitivity of these bands. In the 7-15μm bands we are essentially seeing the entire ULIG population. The behavior of the other components being sim-

Table 2. ASTRO-F Narrow Band Filter Survey Detection Limits.

wavelength	Sensitivity limit (μJy)			
	shallow survey (single pointing)	deep survey ($\approx$ 20 pointings)	source confusion limit Levol model	ULIG model
7μm	20	4	2.7	3.3
9μm	31	7	5.2	7.8
11μm	53	12	9.2	14.5
15μm	85	19	29.9	76
20μm	120	27	83.4	158
25μm	150	34	149.3	363

Table 3. Comparison of ISO and ASTRO-F 15μm Surveys.

Survey Name	Reference	Area	Sensitivity
ISO Lensed	(Biviano et al. 1999)	$56'^2$	$0.07mJy$
HDF	(Serjeant et al. 1997)	$5'^2$	$0.2mJy$
CAM shallow	(Elbaz et al. 1999)	$0.41^{\square}$	$0.8mJy$
CAM deep	(Elbaz et al. 1999)	$0.3^{\square}$	$0.5mJy$
ASTRO-F deep NEP	-	$3200'^2$	$0.04mJy$
ELAIS	(Rowan-Robinson et al. 1999)	$12^{\square}$	$2mJy$
ASTRO-F shallow	-	$18^{\square}$	$0.085mJy$

ilar to the *Levol* model. Once again, significant contribution comes from the PAH features in the ULIG SED at the longer wavelengths. In all wavebands the contribution from the ULIG component peaks at about redshift 1 due to the form of the strong density evolution assumed by the model. Also prominent at 20μm is a double hump in the ULIG number redshift distribution. This feature is prominent due to the evolution incorporated into the ULIG model. In this scenario there is a peak and dip at a redshift ≈1 in the ULIG population corresponding to the redshift of the 9.7μm silicate absorption band observed at 20μm.

4.4 The 18sq. deg. MIR shallow survey

For the case of the ($\approx 18^{\square}$) wide, shallow survey, the aim would be to cover as large an area as possible with the hope of serendipitously discovering new or rare mid-infrared objects. Of course, surveying such a large area in *all* IRC bands would be very time consuming with the same area having to be surveyed over 3 passes of the telescope, one for each of the filter wheel positions of the MIR-L and MIR-S. In reality, it may be that fewer filters (or a wide band filter) will be used. However, we present here the predictions for *all* IRC bands (7-25μm).

In fig. 9 the predicted results for the wide, shallow survey are shown in the same form as the deep NEP survey. Note that again the ultraluminous galaxy component for *Levol* model is not included, although one of the aims of this survey would be the serendipitous discovery of such ultra/hyperluminous objects, with between a few to ∼10 of such objects predicted from 7-25μm respectively.

The number of normal, starburst and AGN galaxies predicted are similar for both evolutionary models with approximately 25,000 starburst galaxies and 35,000 AGN being detected in all bands and the proportion of normal galaxies gradually decreasing towards longer wavelengths. However, the major difference between the *Levol* and *ULIG* evolutionary models is the increasing contribution from and gradual dominance of the ULIG component in the *ULIG* model. This dominance is due to the strong evolution incorporated into the ULIG component peaking at a redshift of ∼1. Note that the results for the 20-25μm bands mirror those of the deep survey and are simply scaled by the increased survey area since both the deep and shallow surveys are source confusion limited. Fig. 10 presents the predictions for the number-redshift (N-z) distributions for the shallow survey. Naturally the N-z distributions for the deep and shallow surveys are quite similar in shape, the number of sources in the shallow survey being scaled by the larger area covered. In general the peaks produced by the PAH features at higher redshifts are weakened with respect to those at lower redshift due to the lower sensitivity of the shallow survey compared to the deep survey. Although in fact at the longest wavelengths (20-25μm) both the deep and shallow surveys would be source confusion limited. It may seem that at these wavelengths a deep survey may seem pointless, although it should be noted that P(D) analysis below the source confusion limit can also yield useful insight into the nature of the sources observed (e.g. (Matsuhara 2000)).

5 IRC SURVEYS WITH WIDE BAND FILTERS

5.1 The Wide Band Filter Option?

There is still one spare position on the ASTRO-F-IRC filter wheels. One interesting option for this spare position would be a wide-band filter encompassing the entire wavelength range of the channel. i.e. a 6-12μm filter for the IRC-MIR-S and a 12-25μm filter for the IRC-MIR-L. The resolution for a central wavelength of 9μm would then be $\Delta\lambda/\lambda_c = 6/9 = 2/3$, thus giving a gain in sensitivity over the narrow filter configuration of $\sqrt{(2/3)/(1/5)} = \sqrt{10/3} \approx \sqrt{3}$. Although the gain in sensitivity is impressive, the associated loss of resolution and colour information must also be considered.

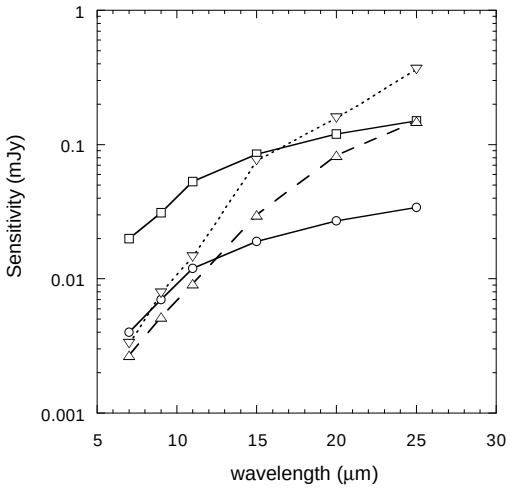

Figure 6. Survey sensitivities at 7, 9, 11, 15, 20 & 25μm shown for the proposed 3200sq.arcmin. deep NEP survey (*circles*), the 18sq.deg. shallow (single pointing) survey (*squares*) and the corresponding source confusion limits predicted by the *Levol* (*up triangles*) and *ULIG* models (*down triangles*). For the deep survey, in general the shorter wavelength observations with the IRC-MIR-S remain above (*Levol* model) or close to (*ULIG* model) the source confusion limit. However the longer wavelength observations with the IRC-MIR-L are expected to be strongly constrained by the confusion due to faint sources. For the wide, shallow survey the sensitivities attainable at longer wavelengths (MIR-L) depend critically on the evolutionary models.

Fig. 3 shows the effect of smoothing the model galaxy SEDs by the wide band filters.

The integral counts at the central wavelengths of 9μm and 18μm for the wide band filter configuration are not immediately visually different from the integral counts calculated using the narrow band filters and hence are not shown here. The sensitivities assumed for both the 3200sq.arcmin. deep NEP MIR survey and ∼18sq. deg. shallow MIR survey using the wide band filters are tabulated in table 4. Also shown are the confusion limits due to faint background sources assuming the *Levol* and *ULIG* models respectively. From our previous investigation of the source confusion limits assuming the narrow band filter configuration (see table 2), it is clearly seen that the severity of the source confusion increases with observing wavelength, the longer wavelengths becoming confused faster than the shorter wavelengths. Therefore, in order to calculate the source confusion limits for the wide band filters we assumed the longest wavelength in the band dominates the source confusion limits, (i.e.12μm for the 6-12μm channel and 25μm for the 12-25μm channel). This would be our worst case scenario for the survey sensitivity. From table 4, it can be seen that there is little or no gain in the sensitivity of the deep survey over the shallow survey, both being basically constrained by the source confusion contamination.

Therefore, for the case of the deep 3200sq.arcmin. NEP MIR survey it would be prudent to use the narrow band filters as they remain (at least for IRC-MIR-S) above the confusion limit and there is little overhead or wasted time in changing the filters as the NEP could be observed easily many times. However for the larger area, shallow 18sq. deg. MIR survey, re-scanning the same area of sky 3 times (1 for each narrow band filter position on the IRC-MIR-S and MIR-L), may produce unreasonable overheads (this is without taking account of the additional scans for redundancy in the observations). Therefore the wide band filters would provide a faster, more economical alternative, with albeit, obvious disadvantages. For consistency, in this paper we discuss both deep and shallow survey wide band filter strategies.

5.2 Wide Band Filter Survey Predictions

In table 5 the predicted results for the deep 3200sq. arcmin. and shallow ∼18sq. deg. survey are shown.

Considering the deep 3200sq. arcmin. NEP survey, the *Levol* model predicts comparable numbers ∼20,000 sources, for both the wide 9μm band and the 9μm & 11μm narrow bands. For the wide 9μm band, assuming the *ULIG* model, approximately 20,000 sources are predicted, compared to ∼25,000 and ∼30000 in the 9μm & 11μm narrow bands respectively. This discrepancy between the models is due to the more severe constraint placed on the *ULIG* model by the confusion due to faint sources. At 18μm, where the constraint due to the source confusion is even more severe, both the *Levol* and *ULIG* models fall short of matching either the narrow band filter 15μm or 20μm predictions. Of course it should be kept in mind that the source confusion limits are set using the long wavelength edge of the wide bands.

However, considering the ∼18sq. deg. shallow survey, there is a shift in favour of the wider band filter configuration. Both the *Levol* and *ULIG* models predict higher numbers of sources in the 9μm wide band than in both the 9μm & 11μm narrow bands. For example, assuming the *Levol* model, approximately 250,000 sources would be expected at 9μm with the wide band filter configuration, compared with the narrow band predictions of ≈100,000 at both 9μm & 11μm. The *ULIG* model similarly predicts twice as many galaxies using the wide band filter configuration. In the case of the large area, shallow survey we are not integrating so deeply and therefore we do not become confusion limited so quickly. Therefore, the increased sensitivity gained in using the wide band filter configuration is not wasted.

In the longer 18μm wide band, both the *Levol* and *ULIG* models predict of the order of 100,000 sources. As was the case before for the longer wavelength filters, confusion is again the limiting factor with the 18μm wide band configuration giving similar results as the longer wavelength filters (20-25μm) in the narrow band filter configuration.

In fig. 11 the predicted number redshift distributions for the 3200sq.arcmin. deep NEP survey are shown for the *Levol* and *ULIG* models respectively. The corresponding results for the shallow survey are not plotted as they are essentially identical, being effectively scaled by the increased area of the survey. The main visible difference between the

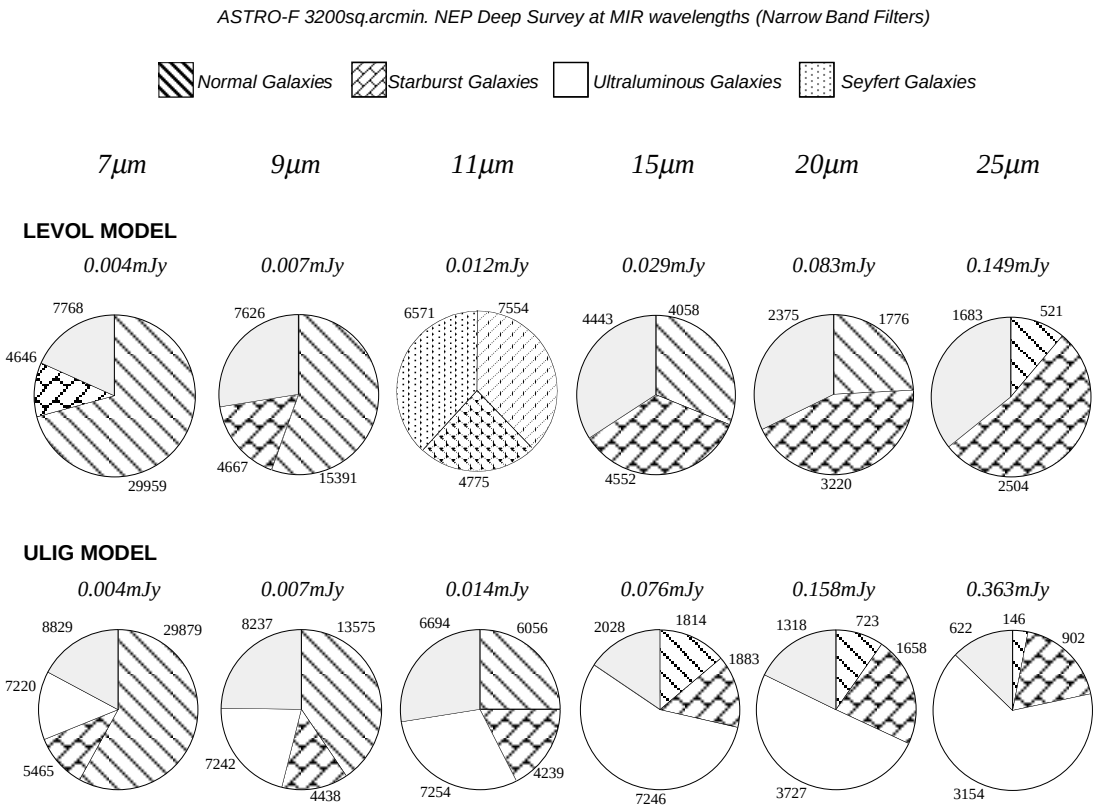

Figure 7. Predicted numbers of galaxies for ASTRO-F deep 3200sq.arcmin. mid-IR survey. Predicted numbers and relative proportions of galaxies for both the Levol model (*top*) and ULIG model (*bottom*) are shown for the respective survey sensitivity limits (in mJy) given in table 2. Note that if the survey sensitivity is source confusion limited then the sensitivity limit is dependent on the evolutionary model. The ultraluminous galaxy component for the *Levol* model is not included in the figures as their numbers are negligible.

Table 4. ASTRO-F Wide Band Filter Configuration Survey Detection Limits.

wavelength	Sensitivity limit (mJy)			
	shallow survey (single pointing)	deep survey ($\approx$ 20 pointings)	source confusion limit Levol model	ULIG model
9μm	0.017	0.004	0.0108	0.0172
18μm	0.055	0.012	0.1210	0.2767

wide band N-z distributions and those of the narrow band is the further *smoothing out* of the influence of the infra-red bands (PAH features) and absorption features. Note that the 9.7μm absorption feature has all but disappeared from the longer wavelength N-z distributions.

5.3 Galaxy Colours and Photometric Redshifts

The mid and far infrared galaxies detected can be used to gain much information on both the galaxy type and evolution. It was on the basis of galaxy colours that the IRAS sources were divided into relatively distinct populations (cirrus, starburst, Seyfert) (Rowan-Robinson & Crawford 1989), (Soifer, & Neugebauer 1991). In the mid-infrared, Fang et al. (1998) used the 25μm sample of Shupe, Fang & Hacking (1998) and the ISO observations of Lu et al. (1997), to calculate the 12/25μm colour-colour diagrams. In general, it was found that using a combination of 12/25μm colour and mid-infrared luminosity at 25μm, the different galaxy populations could be distinguished. For example, the luminous starburst galaxies were found to have systematically redder 12/25μm colours than those of AGN - a powerful discrimination tool. Results from the ISO-ELAIS survey have shown that stars and galaxies in such mid-IR surveys can also be easily discriminated by means of their mid-infrared colours (Crockett et al. 2000).

In fig. 12 we plot the 15/9μm and 25/15μm colour redshift relations for the normal (cirrus type) and starburst galaxy components assuming the *narrow band filter configuration*. Even though the model galaxy SEDs have been smoothed by the filter bandwidth, the contribution from the infrared unidentified bands (PAH features) severely contaminate the colours resulting in erratic switching of the dominant wavelength. This is further exemplified in the 15/9μm - 25/15μm colour-colour diagram. Although in general, the starburst galaxies tend to have warmer 25/15μm colours,

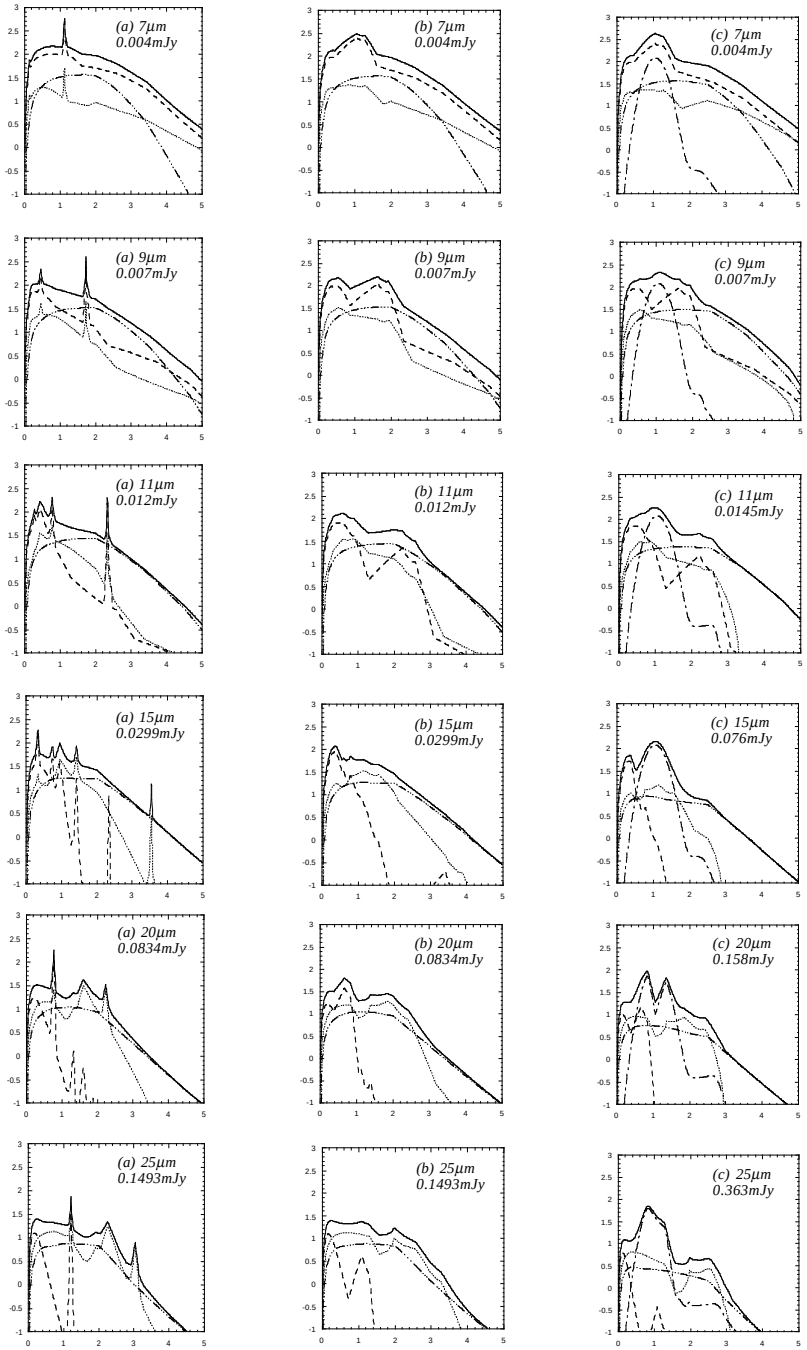

Figure 8. N-z distribution of sources predicted for a deep survey with ASTRO-F around the NEP covering 3200sq.arcmin with survey sensitivities from tab. 2. Vertical axes are (*lg(Number of sources / survey area (sq.deg.))*, horizontal axes are *redshift*. Panel a) N-z distributions using the unsmothed SEDs as spectral templates. Note the prominent spikes caused by the PAH features. Panel b) Results for *Levol* model. Panel c) Results for *ULIG* model. (*solid line*) - All Components, (*dashed line*) - Normal Galaxies, (*dotted line*) - Starburst Galaxies,(*dot-dot-dot-dash line*) - AGN and (*dot-dash line*) - ULIG Galaxies. Note the ULIG contribution in the *Levol* model is too low to be included in the plots.

there is much confusion and overlap between the normal and starburst populations. Furthermore, another motivation for measuring the colours of the observed sources would be to obtain some rough estimate of photometric redshifts. From the 15/9μm - 25/15μm colour-colour diagram, it can easily be seen that such estimations may be extremely difficult.

However, by combining measurements with the IRC-MIR-L (25μm), IRC-MIR-S (9μm) and IRC-NIR (2.2μm) channels, a better distinction can be achieved between both the galaxy populations and their photometric redshifts. Fig 12 also shows the 25/9μm and 9/2.2μm colour redshift relations and the corresponding 9/2.2μm-25/9μm colour-colour diagram. Here we find a better distinction as the introduction of the K-band channel effectively introduces a bimodal

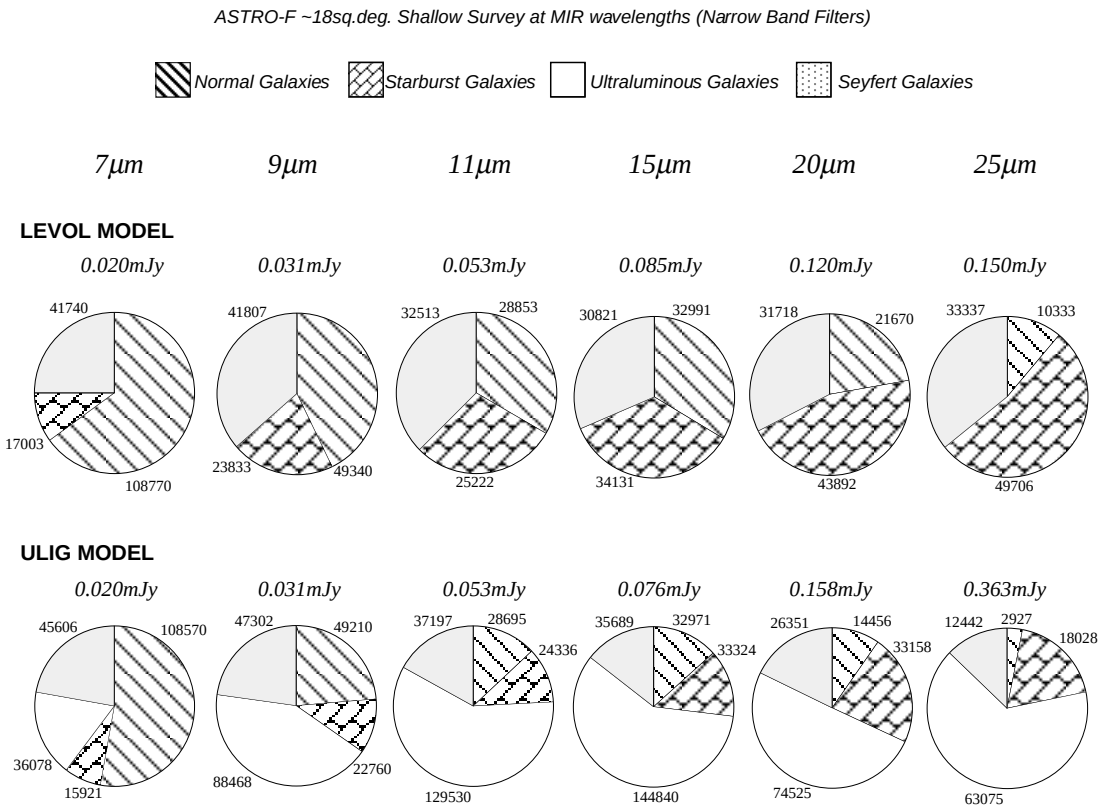

Figure 9. Predicted number of galaxies for ASTRO-F shallow ∼18sq.deg. mid-IR survey. Numbers and relative proportions of galaxies for both the Levol model (*top*) and ULIG model (*bottom*) are shown for the respective survey sensitivity limits (*in mJy* - see table 2). Note that if the survey sensitivity is source confusion limited then the sensitivity limit is dependent on the evolutionary model. The ultraluminous galaxy component for the Levol model is not included in the figures as their numbers are negligible.

Table 5. Survey Predictions Assuming Wide Band Filter Configuration.

Component	Levol Model				ULIG Model			
	Deep		Shallow		Deep		Shallow	
	9μm	18μm	9μm	18μm	9μm	18μm	9μm	18μm
Normal Galaxies	10460	1710	118350	34220	5800	670	115940	13790
Starburst Galaxies	4450	2000	59750	40020	3050	700	60960	14030
Ultraluminous Galaxies	0.3	0.3	5	6	7240	3180	144750	63530
Seyfert Galaxies	5470	1380	74450	27640	4240	540	84850	10850

segregation into the starburst and normal galaxy populations (especially at the highest redshifts) with the normal galaxies generally having cooler 9/2.2μm colours than all but the lowest redshift starburst galaxies. However there is still substantial *contamination* as the unidentified band *PAH forest* is redshifted into the observing bands.

An interesting alternative is to use the wide band filter configuration (combined with one of the IRC-NIR channels e.g. K-band 2.2μm) to obtain colour-colour distributions in the hope that the contamination due to the unidentified bands will be further *washed out*. In fig. 13 the 9/2.2μm-18/9μm colour-colour diagram is plotted. Here we see a striking bimodal distinction between the normal and starburst galaxy components. In general the lower redshift normal galaxies have cooler colours than their starburst counterparts with the higher redshift areas again being completely distinct. It should also be noted from fig. 11 that in the 18μm band there are almost no normal galaxies beyond a redshift of 1, thus further simplifying the colour-colour diagram.

6 SUMMARY AND CONCLUSIONS

We have introduced ASTRO-F (the Imaging Infra Red Surveyor - IRIS) as a next generation infra-red telescope in space. ASTRO-F has both the capability to take extremely deep pointed observations of 100sq.arcmin. regions of the sky in 9 separate wavelength bands from 2.2-25μm at mid and near infrared wavelengths down to sensitivities of an order of magnitude below all but the deepest ISO surveys (see tab.3), at twice the resolution (Watarai et al. 2000).

Two basic survey strategies have been presented. The first, an ultra-deep survey covering ∼ 3200sq.arcmin. in a

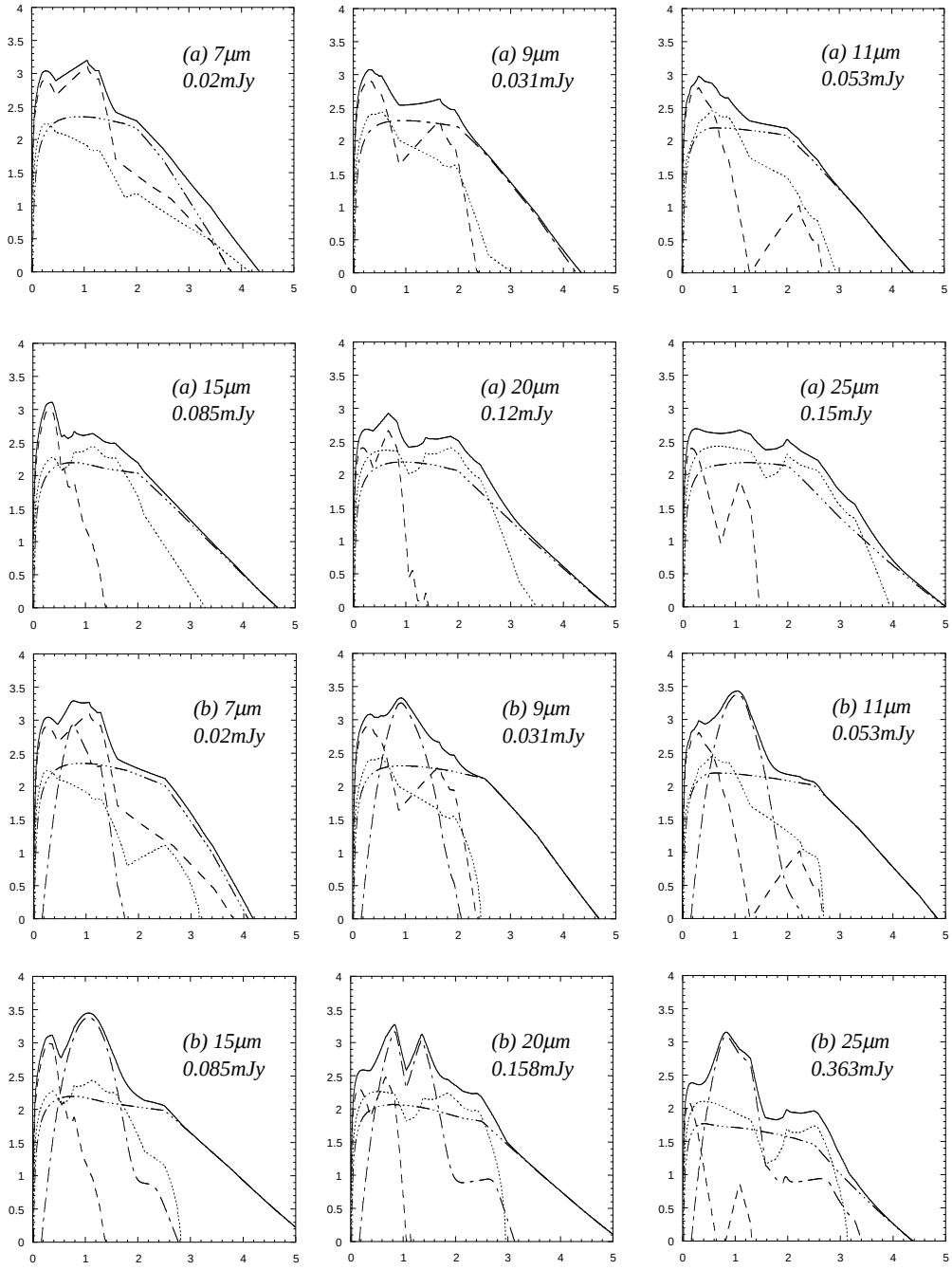

Figure 10. N-z distribution of sources predicted for an 18sq.deg. mIR shallow survey with ASTRO-F with survey limits from table 2. Vertical axes are (*lg(Number of sources / survey area (sq.deg.))*, horizontal axes are *redshift*. Panel a) Results for *Levol* model. Panel b) Results for *ULIG* model.(*solid line*) - All Components, (*dashed line*) - Normal Galaxies, (*dotted line*) - Starburst Galaxies,(*dot-dot-dot-dash line*) - AGN and (*dot-dash line*) - ULIG Galaxies. Note the ULIG contribution in the *Levol* model is too low to be included in the plots.

doughnut around the North Ecliptic Pole and the second a wide area shallow survey covering almost 18sq.deg..

Survey predictions have been made assuming 2 starkly different evolutionary models including normal, starburst, ultraluminous and Seyfert galaxy components. The first is a classic $(1+z)^{3.1}$ pure luminosity evolution (*Levol*) model (Pearson & Rowan-Robinson 1996). The second(*ULIG*) model is a more drastic evolutionary model incorporating a strongly evolving ULIG component (Pearson2000b).

For the deep survey, in general the evolutionary models predict that between 20,000-30,000 sources would be detected in the shortest wavebands dropping to ≈5000 in the longest (25μm) band.

At the longest MIR wavelengths, the deep survey would be severely constrained by the source confusion limit render-

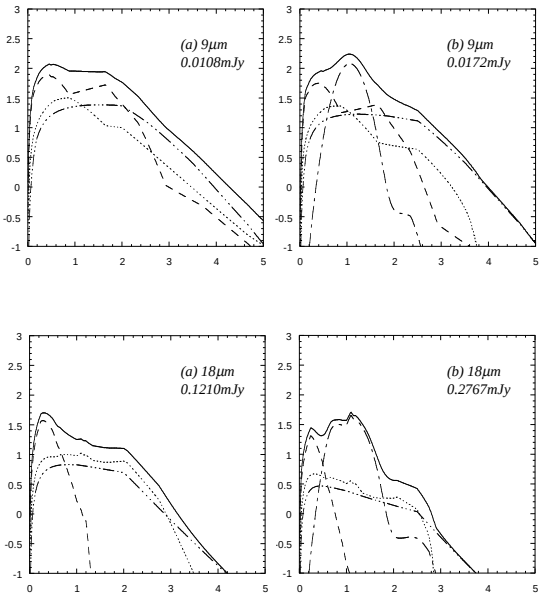

Figure 11. Assuming the wide band filter configuration. 12μm and 18μm N-z distribution of sources predicted for a deep survey with ASTRO-F around the NEP covering 3200sq.arcmin with survey sensitivities from table 4.. Vertical axes are (*lg(Number of sources / survey area (sq.deg.))*, horizontal axes are *redshift*. Panel a) Results for *Levol* model. Panel b) Results for *ULIG* model.(*solid line*) - All Components, (*dashed line*) - Normal Galaxies, (*dotted line*) - Starburst Galaxies,(*dot-dot-dot-dash line*) - AGN and (*dot-dash line*) - ULIG Galaxies. Note the ULIG contribution in the *Levol* model is too low to be included in the plots.

ing the deepest integrations relatively futile, although the simultaneous observations with the IRC-NIR will assist in the source extraction . This will be an important constraint for both the ASTRO-F, SIRTF and future relatively small aperture space infrared telescopes. Although SIRTF has a slightly larger primary (85cm) than ASTRO-F, source confusion at longer mid-infrared wavelengths will still be severe. To integrate deeper *below* the current constraints set by the source confusion, telescopes with significantly larger mirrors will required (Pearson 2000c) (e.g. NGST and the proposed HII/L2 mission (Nakagawa et al. 1998)).

In the shorter wavelength bands it should be possible to detect many sources out to high redshift ~ 5 with more than half of the normal galaxies being at redshift >1 in the 7 & 9μm bands. Without doubt the infrared unidentified bands (UIB - PAH features) in the observed galaxy spectra aid in the detection of galaxies to higher redshift, with the 3.3μm feature enhancing the detectabilty of normal galaxies out to high redshift and the PAH *forest* in general enhancing the detectability of all starforming and normal galaxies in the 20μm band.

The large area, 18sq.deg., shallow survey would produce between 150,000 sources in the shortest waveband to 100,000 sources in the longest waveband. In this case, source confusion is not so much of a problem as only a single pointing is made at each position. Note that a single pointing corresponds to 42-60 individual frames. Therefore there is intrinsic redundancy to distinguish real detections from those of spurious events such as cosmic ray hits which can have a severe effect on IR observations e.g. Aussel et al. (1999)). However, if the stronger evolving *ULIG* model is assumed then even a shallow survey will be source confused to some extent at the longest MIR wavelengths (20-25μm).

The orbit of ASTRO-F is naturally conducive to the NEP deep survey, allowing many chances of observation every orbit. Where as the shallow area survey would require multiple passes of the same area to allow observations at all wavelengths (i.e. 3 passes). This may incur intolerable overheads. Such overheads could be reduced by using the filters in such a combination as to minimize waste, i.e. 25μm + 11μm, 20μm + 9μm, 15μm + 7μm. In a further response to this problem we have investigated the possibility of using the *spare* positions on the IRC-MIR-S and IRC-MIR-L filter wheels as additional *wide band* filters at 9μm and 18μm respectively. Although there is a gain in sensitivity in using these wider band filters, this would be lost on the deep survey as the confusion noise is already above or close to the detection limits. For the shallow survey we find that using this wide-band filter configuration leads to a higher or similar number of detections in the 9μm and 18μm respectively.

Using colour-colour plots we should be able to distinguish between different galaxy populations and also obtain rough photometric redhifts if the MIR-S and MIR-L observations are combined with an additional observation using the IRC-NIR channel at 2.2μm.

During its $\sim$ 500 day lifetime (defined by the estimated time of Helium exhaustion), ASTRO-F should make of the order of 7400 pointed observations with the IRC instrument. Of these up to; 32x20 (NEP survey) x 3 (narrow bands filters) + 32x20 (shallow survey) x 2 (wide band filters) = 3200 pointings (or more) could be invested into MIR surveys (since ASTRO-F is in essence a survey mission). Such surveys would approximately double the current area surveyed in the mid-IR (with ISO) and reach to extremely deep fluxes. Following the same doctrine as the ISO 15μm surveys (Elbaz et al. 1998), ASTRO-F could produce a number of mid-IR surveys covering a wide spectrum of sensitivities and spatial areas. In addition, follow up observations with both the IRC (including spectroscopy) and from the ground, would provide extremely detailed information over the entire MIR wavelength range as to the nature of all types of galaxies in the infrared. Finally it is hoped that ASTRO-F and SIRTF will complement each other and pave the way for future generations of space telescopes in the near & mid-infrared (NGST, HII/L2).

7 ACKNOWLEDGEMENTS

The ASTRO-F project is managed and operated by the Institute of Space and Astronomical Science (ISAS) Japan in collaboration with the groups in universities and institutes in Japan. We are grateful for all the members of the ASTRO-F project for their efforts and support. The authors would like to thank the anonymous referee for many useful sugges-

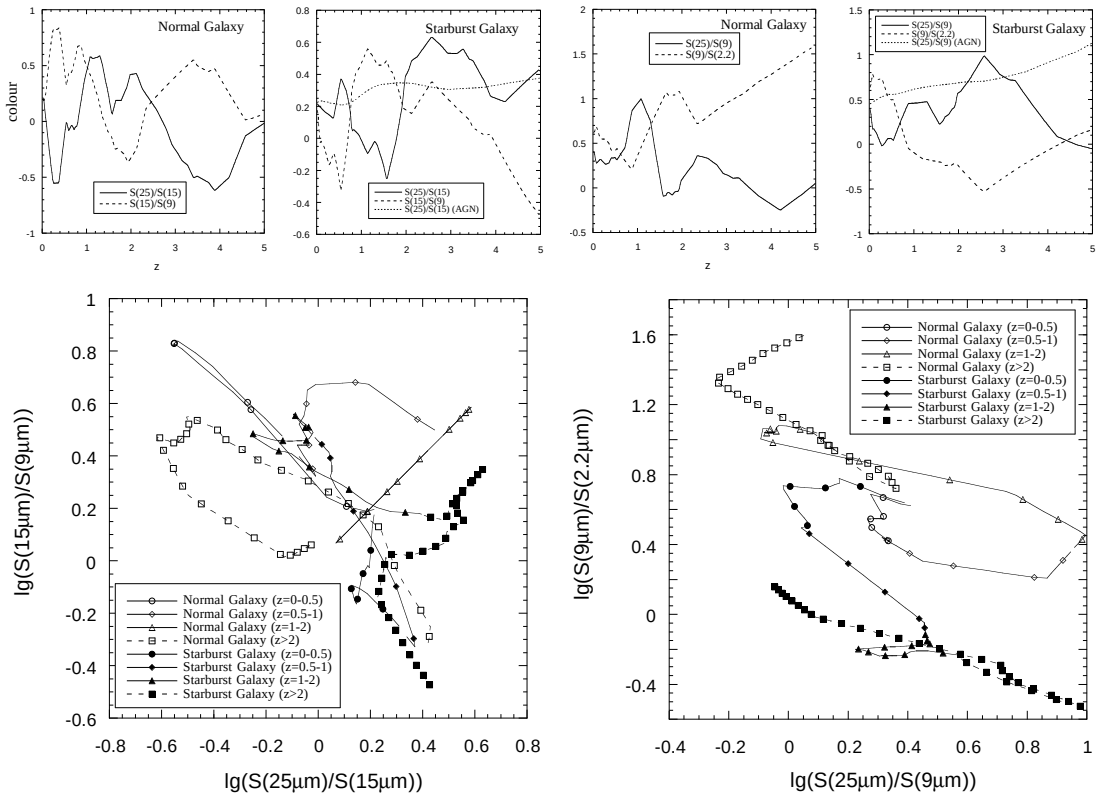

Figure 12. Top panels - Colour-redshift distributions for normal and starburst galaxies (and AGN) assuming the narrow band filter configuration at 25, 15, 9 & 2.2μm. Bottom panels - The 15/9μm - 25/15μm (left) and 9/2.2μm-25/9μm (*right*) colour-colour diagrams for normal (*unfilled markers*) and starburst (*filled markers*) galaxies. The results are divided into redshift regimes as described in the legend with each marker denoting 0.1 in redshift.

tions that greatly improved the clarity of this paper. CPP is supported by a Japan Society for the Promotion of Science (JSPS) fellowship.

REFERENCES

Acosta-Pulido J.A. et al., 1996, AA, 315, 121
Altieri B. et al., 1999, AA, 343, L65
Aussel H., Cesarsky C.J., Elbaz D., Starck J.L., 1999, AA, 342, 313
Barger A.J.,Cowie L.L., Sanders D.B., 1999, ApJ, 518, L5
Benn C.R., Rowan-Robinson M., McMahon R.G., Broadhurst T.J., Lawrence A., 1993, MNRAS, 263, 98
Biviano et al., 1999, In: Mezure A., Le Fevre O., Le Brun V., (Ed.)Clustering at High Redshifts,ASP Conference series, 2000, astro-ph/9910314
Blain A.W.,Kneib J.-P., Ivison R.J., Smail I., 1999, ApJ, 512, L87
Bogun S. et al., 1996, AA, 315, L71
Boulade O., 1996, AA, 315, L85
Boyle N., Shanks T., Peterson B.A., 1988, MNRAS, 235, 935
Crockett H. et al. 2000, MNRAS, in preparation
Dole H. et al. 2000, In: Lemke D, Stickel M.K. (Ed.)ISO Surveys of a Dusty Universe, Springer–Verlag, 54
Efstathiou A., Rowan-Robinson M., Siebenmorgen R., 2000, MNRAS, *accepted*
Efstathiou,A.,Siebenmorgen,R., 2000, MNRAS, 313, 734
Elbaz D. et al., 1998, in Proc. of 34th Liege International Astrophysics Colloquium on the "Next Generation Space Telescope", Belgium, June 1998, astro-ph/ 9807209v2
Elbaz D. et al., 1999, AA, 351, L37
Elbaz D., 1999b, In: F.Hammer, T.X.Thuan, V.Cayette, B.Guideroni, J.Tran Thuan Van (Eds.) Building the Galaxies from the Primordial Universe to the Arcs, XIX Moriand Astrophysics Meeting, March 1999, eds. frontieres. astro-ph/9911050
Fang F., Shupe D. L., Xu C., Hacking P. B., 1998, ApJ, 500, 693
Fazio G.G. et al., 1998, In: Fowler A.M. (Ed.)Infrared Astronomical Instrumentation, Proc. SPIE 3354, 114
Flores H.et al., 1999a, ApJ, 517, 148
Flores H. et al., 1999b, AA, 343, 389
Genzel R. et al., 1998, ApJ, 498, 579
Goldschmidt P. et al., 1997, MNRAS, 289, 465
Hughes D. et al., 1998, Nature, 394, 241
Kawara K. et al., 1998, AA, 336, L9
Kawada M., 1998 In: Fowler A.M. (Ed.)Infrared Astronomical Instrumentation, Proc. SPIE 3354, 905
Kessler M., et al., 1996, AA, 315, L27
Kim D.C., Sanders D.B., 1998, ApJS, 119, 41
Lawrence A., Walker D., Rowan-Robinson M., Leech K.J., Penston M.V., 1986, MNRAS, 219, 687
Lindern-Vørnle M. J. D. et al., 2000, astroph/0005354
Lu N.Y.et al., 1996, BAAS, 28, 1356
Lutz D. et al, 1997, A&ASS, 248, 217
Madau P., Ferguson H. C., Dickenson M. E., Giavalisco M., Steidel C., Fruchter A., 1996, MNRAS, 283, 1388
Matsuhara H., 1998, In: Fowler,A.M. (Ed.)Infrared Astronomical Instrumentation, Proc. SPIE 3354, 915

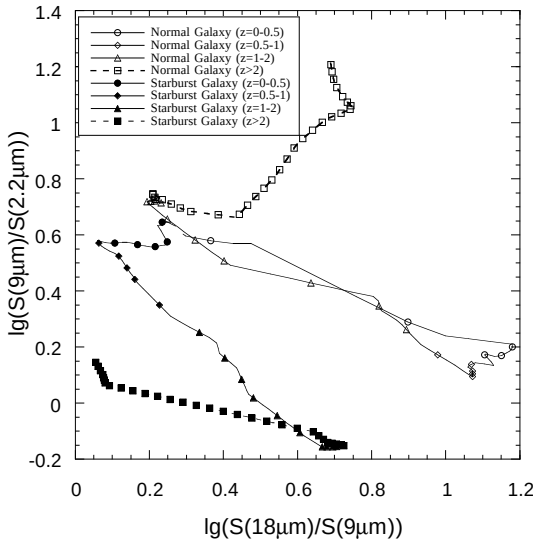

Figure 13. The 9/2.2μm - 18/9μm colour-colour diagrams for normal (*unfilled markers*) and starburst (*filled markers*) galaxies assuming the wide band filter configuration. The results are divided into redshift regimes as described in the legend with each marker denoting 0.1 in redshift. Note that although in practice the variance in the individual galaxy colours will cause a *smudging* in the colour-colour plane, the substantial separation between the 2 populations should still remain.

Matsuhara H. et al., 2000, AA submitted
Matsumoto T. et al, 2000, In: Lemke D, Stickel M.K. (Ed.)ISO Surveys of a Dusty Universe, Springer–Verlag, 99
Metcalfe L.et al., 1999, In: Cox P., Kessler M. (Ed.) The Universe as seen by ISO, astro-ph/9901147
Murakami H. et al, 1996, PASJ, 48, No.5-6
Murakami H., 1998, In: Bely P.Y., Breckinridge J.B. (Ed), Space Telescopes and Instruments, Proc. SPIE 3356, 471
Nakagawa T. et al., 1998, In: Bely P.Y., Breckinridge J.B. (Ed), Space Telescopes and Instruments, Proc. SPIE 3356, 462
Oliver S.J. et al., 1997, MNRAS, 289, 471
Oliver S.J. et al., 2000a, MNRAS, 316, 749
Oliver S.J. et al., 2000b, In: Lemke D, Stickel M.K. (Ed.)ISO Surveys of a Dusty Universe, Springer–Verlag, 29
Onaka T.,Sugiyama Y.,Miura S., 1998, In: Fowler A.M. (Ed.)Infrared Astronomical Instrumentation, Proc. SPIE 3354, 900
Pearson C.P.,Rowan-Robinson M. 1996, MNRAS, 283, 174
Pearson C.P., 2000a, In: Lemke D, Stickel M.K. (Ed.)ISO Surveys of a Dusty Universe, Springer–Verlag, 149
Pearson C.P., 2000b, MNRAS, astro-ph/0011335
Pearson C.P., 2000c, In: Matsumoto T., Shibai H.(Ed.) Mid- and Far-infrared Astronomy and Future Space Missions,ISAS Report Special Edition (SP No.14)
Pearson C.P., in preparation,
PugetJ.L., Leger A., 1989, ARAA, 27, 161
PugetJ.L. et al., 1996, AA, 308, L5
Rieke G.H., 2000, In: Lemke D, Stickel M.K. (Ed.)ISO Surveys of a Dusty Universe, Springer–Verlag, 403
Roache P.F., Aitken D.K., Smith C.H., Martin J.W., 1991, MNRAS, 248, 606
Rowan-Robinson M., Crawford P. 1989, MNRAS, 238, 523
Rowan-Robinson M. et al., 1991, Nature, 351, 719
Rowan-Robinson M., 1992, MNRAS, 258, 787
Rowan-Robinson M., Efstathiou A., 1993, MNRAS, 263, 675
Rowan-Robinson M., Efsthiou A.,Lawrence A., Oliver.S., Taylor .A., 1993, MNRAS, 261, 513
Rowan-Robinson M., 1995, MNRAS, 272, 737
Rowan-Robinson M. et al., 1999, astro-ph/9906273
Rush B., Malkan M., Spinoglio L., 1993, ApJSS, 89, 1
Sanders D.B., Mirabel I.F., 1996, ARAA, 34, 725
Saunders W., Rowan-Robinson M., Lawrence A., Efstathiou G., Kaiser N., Ellis,R.S., 1990, MNRAS, 242, 318
Serjeant S.B.G. et al., 1997, MNRAS, 289, 457
Serjeant S.B.G. et al., 2000, MNRAS, 316, 768
Shupe D. L., Fang F., Hacking P. B., 1998, ApJ, 501, 597
Siebenmorgen R., Krugel,E., 1992, AA 259, 614
Smail I., Ivison R.J.,Blain A.W., 1997, ApJ, 490, L5
Soifer B. T. et al., 1987, ApJ, 320, 238
Soifer B. T, Neugebauer G., 1991, AJ, 101, 354
Takahashi H. et al., 2000, In: Breckinridge J.B. (Ed), UV, Optical, and IR Space Telescopes and Instruments, Proc. SPIE 4013 in press
Taniguchi et al., 1997, AA, 328, L9
Takeuchi T.T., Hirashita H., Ohta K., Hattori G.T., Ishii T.T., Shibai H., 1999, PASP, 111, 288
Vigroux L. et al., 1996, AA, 315, L93
Watarai H. et al., 2000, In: Breckinridge J.B. (Ed), UV, Optical, and IR Space Telescopes and Instruments, Proc. SPIE 4013 in press
Xu,C et al. 1998, ApJ, 508, 576

This paper has been produced using the Royal Astronomical Society/Blackwell Science LaTeX style file.